Light-Triggered Biocatalysis Using Thermophilic Enzyme—Gold Nanoparticle Complexes

Matthew D. Blankschien,[†,‡,¶] Lori A. Pretzer,[§,¶] Ryan Huschka,[§,△] Naomi J. Halas,[‡,§,⊥,∥,#,△] Ramon Gonzalez,[†,‡,#,*] and Michael S. Wong[†,‡,§,▽,*]

[†]Department of Chemical and Biomolecular Engineering, [‡]Richard E. Smalley Institute for Nanoscale Science and Technology, [§]Department of Chemistry, [⊥]Department of Electrical and Computer Engineering, [∥]Department of Physics and Astronomy, [#]Department of Bioengineering, [△]Laboratory for Nanophotonics and the Rice Quantum Institute, [▽]Department of Civil and Environmental Engineering, Rice University, 6100 Main Street, Houston, Texas 77005-1892, United States. [¶]These authors contributed equally to this study.

ABSTRACT The use of plasmonic nanoparticle complexes for biomedical applications such as imaging, gene therapy, and cancer treatment is a rapidly emerging field expected to significantly improve conventional medical practices. In contrast, the use of these types of nanoparticles to noninvasively trigger biochemical pathways has been largely unexplored. Here we report the light-induced activation of the thermophilic enzyme *Aeropyrum pernix* glucokinase, a key enzyme for the decomposition of glucose *via* the glycolysis pathway, increasing its rate of reaction 60% with light by conjugating the enzyme onto Au nanorods. The observed increase in enzyme activity corresponded to a local temperature increase within a calcium alginate encapsulate of ~20 °C when compared to the bulk medium maintained at standard, nonthermophilic temperatures. The encapsulated nanocomplexes were reusable and stable for several days, making them potentially useful in industrial applications. This approach could significantly improve how biochemical pathways are controlled for *in vitro* and, quite possibly, *in vivo* use.
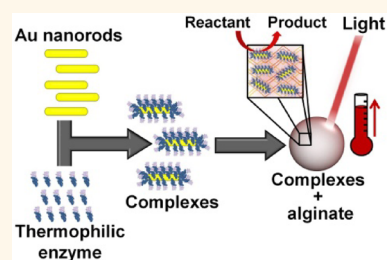
Gold (Au) nanoparticles have been used in a wide variety of biological applications to date, including drug/oligonucleotide delivery, bioimaging, gene therapy, and photothermal therapy.[1−6] The most prominent properties of Au nanoparticles that can be exploited to achieve these applications are their ease of surface functionalization, their biocompatibility, and their surface plasmon-derived optical properties.[1,7,8] Plasmonic Au nanoparticles such as Au nanorods (NRs) have collective electronic oscillations that can be utilized to convert optical energy to thermal energy with high efficiency upon resonant optical illumination.[7,9] This photothermal response is tunable, based on nanoparticle size and geometric configuration, and is particularly important for biological applications because the particles can be designed to have an absorption efficiency in the near-infrared region (NIR) (690−900 nm).[8] Biological reactions and cells are maximally transparent in this "water window", and light can penetrate to depths of several centimeters, even in more complex tissues.[10]

Thermophilic enzymes are obtained from thermophiles, archaea, or eubacteria that thrive at high temperatures (*i.e.*, 50−120 °C).[11] These organisms survive due to proteins that have been highly selected for robust functioning in this elevated temperature range. Many thermophilic enzymes are heat responsive; in other words, they have dramatically lower activity at ambient temperatures than standard enzymes and increase in function up to or beyond their native temperature(s). When combined with plasmonic nanoparticles, the resulting enzyme—nanoparticle complex should be light-triggerable: the local heating induced by resonant illumination of the nanoparticle will activate the attached heat-responsive enzymes.

Currently, control of biochemical pathways, *in vivo* or *in vitro*, is largely achieved by the addition of chemical/biochemical signals or constituents that are difficult to remove once added.[12] Biomolecule—nanoparticle complexes that are designed to be responsive to light could provide an easy means of controlling a biochemical
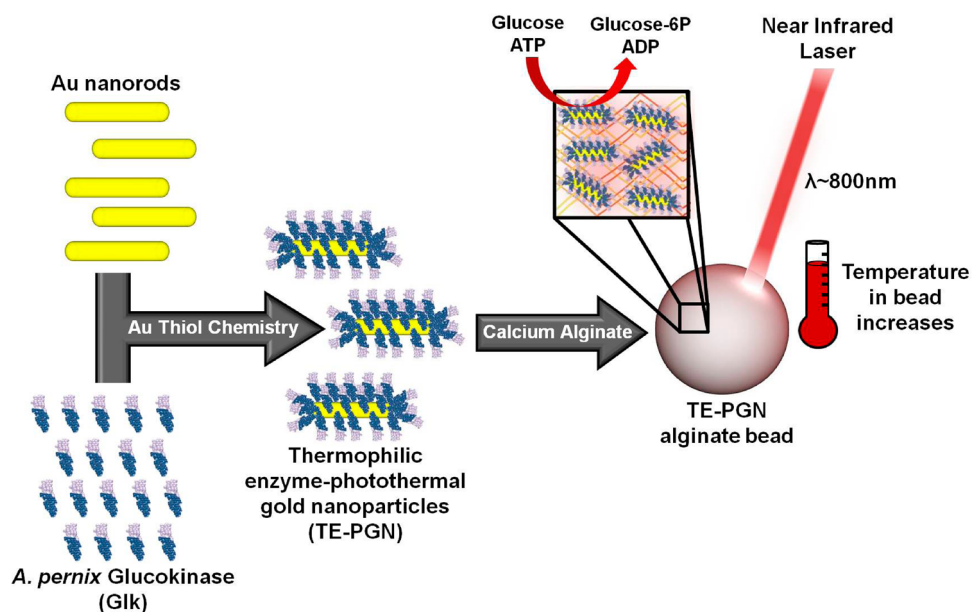
Figure 1. Schematic of thermophilic enzyme−photothermal gold nanoparticle (TE-PGNs) synthesis and laser-induced activation.

reaction in a less intrusive manner than traditional biochemical signals, simply by illuminating with an appropriate light source. To turn off the reaction, one would simply remove the light. This latter attribute is a critical feature, since the remote control of biological reactions could be useful in a multitude of applications. Potential uses would include minimizing operations for industrial biological products or modulating biochemical pathways *in vivo* for therapeutic outcomes. With current conventional approaches, the use of chemical/biochemical signals to control reaction rates can be invasive, more readily introducing contaminating agents such as certain gases or infectious particles into the reactor or resulting in the unwanted synthesis of dangerous byproducts. Indeed, remote control of biological systems inside or outside of cells through the use of nanotechnology has been a novel and exciting forefront of recent studies.[13−17]

In this study, we describe the fabrication of light-responsive, thermophilic enzyme−photothermal gold nanoparticle complexes (TE-PGNs) useful for the light-dependent activation of a biochemical reaction under traditional bulk reaction temperatures (∼20−50 °C). This extends previous studies involving confined heating of DNA with nanoparticles[18,19] and is in direct contrast to recent studies, including elegant ones employing the use of magnetic nanoparticles and magnetic fields that activate biochemical pathways through bulk heating.[13,16,17] The goal here is to minimize such bulk heating so that we can provide proof of concept that could eventually lead to remote triggering of biochemical reactions under standard nonthermophilic conditions utilizing thermophilic enzyme nanoparticle complexes. Our particles consist of a Au nanoparticle core with a monolayer coating of thiol-conjugated

heat-responsive enzyme. Au NRs (∼30 × 10 nm) were chosen for their optical response in the desired "water window" (800 nm), while our chosen model thermophilic enzyme is *Aeropyrum pernix* glucokinase (Glk), a key enzyme in sugar degradation *via* the glycolysis pathway in bacteria and eukarya.[20] The TE-PGNs were encapsulated in a calcium alginate matrix to sequester the heat generated by the Au NR cores excited by a continuous wave laser, such as those used in medical practice. As a result, a temperature gradient sufficient to increase the temperature in the nanometer scale vicinity of the enzyme and activate it without significantly affecting the bulk temperature of the system is formed. The concept of light-dependent activation of a biochemical reaction utilizing our novel encapsulated thermophilic enzyme−photothermal gold nanoparticles is demonstrated in Figure 1.

Gold−thiol chemistry provides both a robust and highly convenient means of binding thermophilic enzymes to Au nanoparticles, with high bond strengths of ∼45 kcal/mol and thermal resistances well past 100 °C.[21] It is already well known that Au nanoparticle surfaces can be readily functionalized with a wide variety of thiolated molecules including oligonucleotides,[1] chemotherapeutic agents,[22] and polypeptides.[23] Attachment is as straightforward as mixing reduced sulfur moieties with the nanoparticles. While many types of functional Au nanocomplexes have been reported, including those with proteins, attachment of a heat-responsive (thermophilic) enzyme has not previously been reported.

RESULTS

Cloning, Purification, and Characterization of *A. pernix* Glucokinase (*glk*). The model thermophilic enzyme we
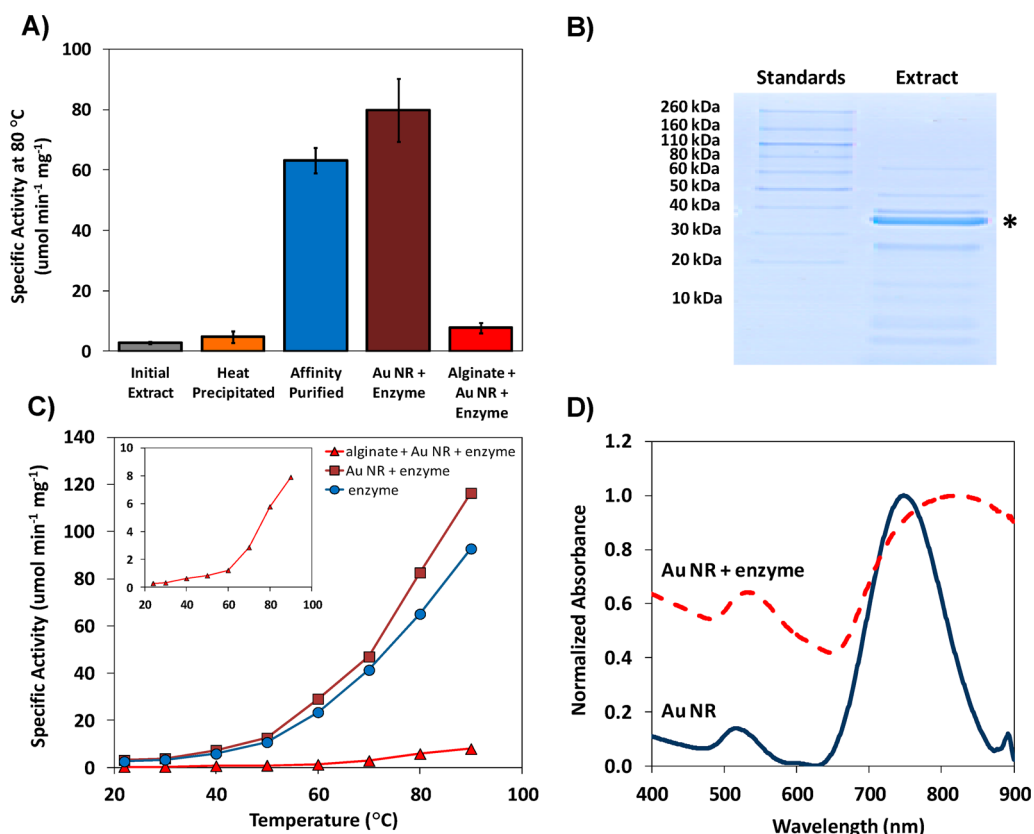
Figure 2. Thermal characterization of purified and TE-PGN-conjugated *A. pernix* glucokinase activity. (A) Specific Glk[AP] activity at 80 °C for successive stages of enzyme purification, after TE-PGN formation (Au NR + enzyme), and of Ca-alginate-encapsulated TE-PGNs. Error bars denote standard deviation of 3 replicates each. (B) SDS-PAGE showing purity of *A. pernix* glucokinase (Glk[AP], 35.19 kDa) in extracts after Ni^{2+} affinity chromatography. (C) Specific activity *vs* bulk temperature kinetics of Glk[AP] either nonconjugated (circles), in TE-PGNs (squares), or in Ca-alginate-encapsulated TE-PGNs. Inset displays the encapsulated TE-PGN data at a smaller scale. (D) UV–vis absorbance spectra of Au NRs (Au NR) and TE-PGNs (Au NR + enzyme).

chose to use in this proof of principle study is the *A. pernix* glucokinase.[20] Glucokinase can serve as an initial and key enzyme (glucose + ATP → G6P + ADP) in glucose degradation *via* the glycolysis pathway found in nearly all bacteria and eukarya, including humans.[24] Besides its central position in an important metabolic pathway, *A. pernix* glucokinase has many ideal characteristics that permit its use in creating TE-PGNs, including: O_2 insensitivity, monomeric character, excellent heat response and very high temperature resistance, low sulfur content, stability in reducing agents, the ability to be heated and cooled repeatedly, and the ability to harbor N-terminal modifications[20] (demonstrated in this study).

Genomic DNA of *A. pernix* was obtained, and the glucokinase (*glk*) gene was PCR (polymerase chain reaction) amplified. The forward PCR primer contained additional coding information for an optimal ATG start codon, a His6 tag, and a sulfur-containing cysteine (Cys) residue. These latter elements would permit affinity purification on Ni^{2+} columns and N-terminal gold–thiol attachment, respectively. The *cyshis₆glk*[AP] PCR product was subsequently cloned into pET28a vector and expressed in an appropriate *E. coli* host. Cell extracts were prepared *via* cell disruption in the presence

of β-mercaptoethanol to maintain reduced sulfur groups (cysteines) for later gold–thiol chemistry. Subsequently, the heat precipitation of native nonthermophilic *E. coli* proteins and metal ion affinity purification utilizing the His6 tag were performed. As seen in Figure 2A (middle column), a high specific activity (μmol mg^{-1} min^{-1} for glucose-6P formation) at 80 °C was obtained after the affinity purification step.

While the heat precipitation step did not yield large increases in purification, it had the added benefit of inactivating native proteases that could inhibit TE-PGN activity in subsequent use. In agreement with the activity obtained after Ni^{2+} affinity chromatography, SDS-PAGE showed that the major polypeptide constituent in the purified extract was at or near the 35.19 kDa expected size of the Cys-His6-Glk[AP] protein (for ease referred to as Glk[AP] hereafter) (Figure 2B). Furthermore, the affinity-purified Glk[AP] displayed the desired heat responsiveness for TE-PGN synthesis, with lower activity from room temperature to ~50 °C, where larger exponential increases occur in response to rising temperatures (Figure 2C). It was observed that Glk[AP] was not active at 4 °C and the observed kinetics were nearly identical to those previously reported.[20] With adequate purity of Glk[AP] achieved, this final extract was

used in the functionalization of Au NRs to create thermophilic enzyme–photothermal gold nanoparticles.

Attachment of Glucokinase to Au NRs and Characterization of the Resulting Conjugates. Au NRs (33 nm × 10.4 nm) were fabricated by standard wet chemistry methods and functionalized with thermophilic Glk^{AP} polypeptides *via* gold–thiol bond formation. The cleaned Au NRs were incubated with the reduced Glk^{AP} extract overnight at room temperature. After centrifugation and washing the resulting pellet to remove all free, unbound enzyme, the TE-PGNs were resuspended by brief sonication and diluted so that the absorbance at 800 nm for a 1/6 dilution was 1.1. The concentration of the NRs in the TE-PGN suspension was $(4.2 \pm 0.06) \times 10^{12}$ NRs/mL, calculated using the average NR dimensions from transmission electron microscopy (TEM) and total Au concentration in the TE-PGN suspension measured *via* inductively coupled plasma optical emission spectroscopy (ICP-OES). A protein loading efficiency of $20 \pm 4\%$ was achieved, resulting in a TE-PGN protein concentration of 0.210 ± 0.02 mg/mL. With these concentrations and an Au NR surface area of ~1250 nm^2, around 850 Glk^{AP} polypeptides (35.19 kDa) are conjugated to the Au NR surface. This agrees with theoretical calculations assuming average specific protein density (0.73 cm^3/g),[25] cubic geometry or spherical geometry, and a linear N-terminus linker of 10 to 20 amino acids (*i.e.*, Cys-His$_6$ residues) for 100% surface coverage with protein.

Characterization of the localized surface plasmon resonance shift (LSPR) of the Au NRs before and after protein functionalization was performed by UV–vis spectroscopy, and the extinction spectra of TE-PGNs and Au NRs in solution are shown in Figure 2D. The large LSPR shift observed is consistent with a dense protein monolayer functionalized to the Au NR surface.

While the resonance wavelengths for the transverse plasmon are similar to that for Au NRs and the TE-PGNs (~520 nm), the higher longitudinal resonance wavelength (~750–850 nm, from the increased aspect ratio) is substantially broader/flatter for the TE-PGNs. This broadening of the longitudinal resonance wavelength and overall increase in absorbance could be due to electronic coupling between the TE-PGNs at the longitudinal wavelength and/or to some aggregation of TE-PGNs in suspension. Indeed, over time, the TE-PGNs are observed to visibly aggregate; however, this is easily reversed by gentle vortexing prior to use.

Thermal, nonlaser testing of these novel thermophilic enzyme–photothermal gold nanoparticles revealed robust specific activity. At 80 °C, the TE-PGNs displayed ~20% greater specific glucose phosphorylation activity than the unbound free enzyme (Figure 2A, for assay see Methods). This increased activity was also evident in the activity *vs* temperature profile, where the TE-PGNs displayed similar enzymatic kinetics to the unbound Glk^{AP} (Figure 2C). The increased specific

activity of the TE-PGNs could reflect a gold–thiol binding selection for more properly folded Glk^{AP} among the total pool of Glk^{AP} and minor contaminating polypeptides. Another possibility is that Au NR-bound Glk^{AP} *vs* unbound enzyme could more readily adopt the right conformation for activity in response to heat by virtue of being conjugated to a scaffold.

Encapsulation of TE-PGNs in Ca-Alginate Matrix. To make the TE-PGNs compatible with continuous wave (CW) laser excitation, we encapsulated concentrated amounts of TE-PGNs in a Ca-alginate matrix to sequester the complexes and enhance the temperature gradient between the nanoparticle–enzyme complex and the bulk solution. Enzyme entrapment within a calcium alginate gel is recognized as a versatile method for not only enhancing stability but also allowing enzyme reuse and separation from the reaction mixture.[26–28]

To encapsulate the complexes, 1.5% w/v sodium alginate and the TE-PGNs were mixed in a 1:1 ratio and dropped in 10 μL aliquots into a solution of 0.5 M CaCl$_2$. This resulted in consistent and uniform TE-PGN Ca-alginate beads (average diameter =1.9 $\pm$ 0.1 mm) easily visible due to their crimson color (Figure 3A).

Scanning electron microscopy (SEM) revealed the TE-PGN-loaded Ca-alginate beads were indeed porous (Figure 3A), with a pore size of a few μm instead of 10–30 nm;[28,29] however, it is possible that the pores were enlarged due to changes induced during sample preparation prior to imaging. This larger-than-expected enhanced porosity could be advantageous since porosity is critical for the transfer of reactants and products to and from the TE-PGNs. Thermogravimetric analysis revealed that ~90 wt % of the beads consisted of water, which agrees with the porosity seen in the SEM analysis (Figure S1).

The TE-PGN alginate beads (5 beads/rxn) were enzymatically active under bulk heating, with the glucokinase specific activity displaying the expected heat-responsive kinetics (Figure 2A, C). The specific activity was ~8-fold lower than the unencapsulated TE-PGNs, which may well be due to the mass transfer limitations of the Ca-alginate matrix. Possible heat transfer limitations into the matrix could also be a factor, as the Ca-alginate encapsulation was performed to reduce bulk heat flow and sustain high temperatures at the TE-PGNs (see below). This lowered specific activity would not be critical for industrial use since this limitation would be offset by the benefit of repeated enzyme bead use. To test reusability, TE-PGN stability and reuse were examined over a 3-day period, and no significant change in enzyme activity was observed (Figure 3B). Furthermore, the TE-PGN alginate beads retained their color, shape, and consistency over multiple weeks, further suggesting their stability and reuse potential.

Laser-Dependent Activation of the Encapsulated TE-PGNs. To test whether TE-PGN complexes could control a
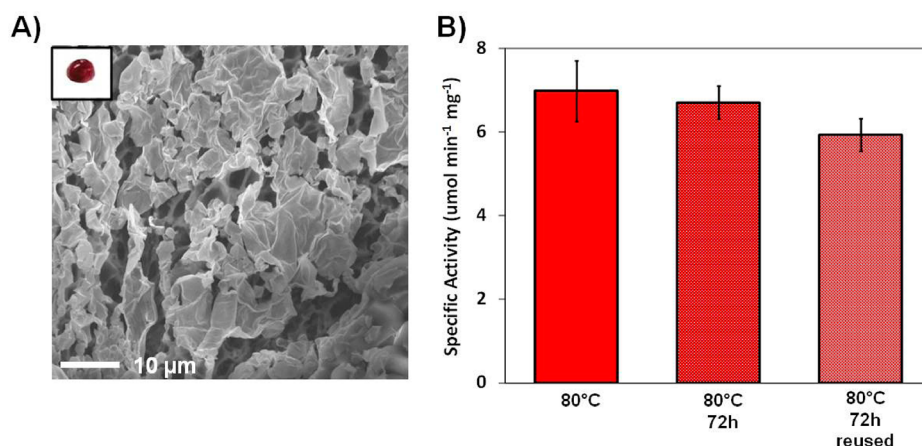
A)

B)

Figure 3. Characterization of thermophilic enzyme−photothermal gold nanoparticles encapsulated in a Ca-alginate matrix. (A) Scanning electron microscopy (SEM) image of the TE-PGN Ca-alginate bead surface. Inset shows visual image of LTNB Ca-alginate bead. (B) Specific Glk^{AP} activity of the LTNB Ca-alginate beads at 80 °C for freshly prepared beads vs untested and reused beads 72 h later. Error bars denote the standard deviation of 3 replicate experiments.
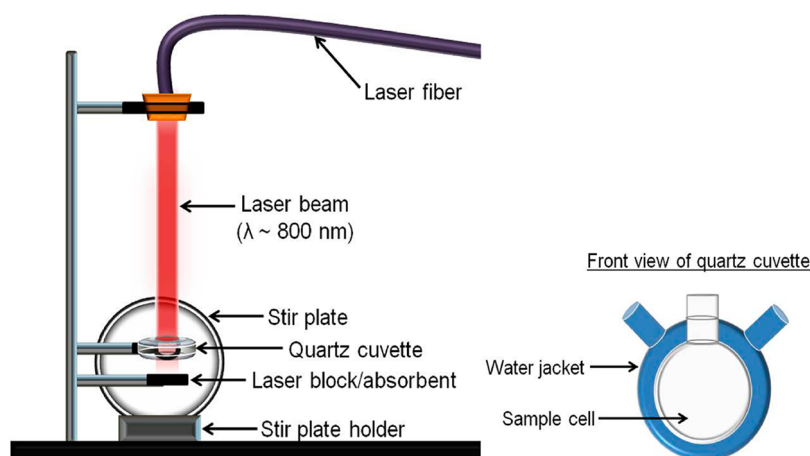

Figure 4. Schematic of laser setup used in this study (further details in the Methods section).

biochemical reaction *via* light activation while maintaining standard nonthermophilic bulk temperatures, the experimental geometry diagrammed in Figure 4 was employed (see also Methods).

Laser treatment consisted of placing 5 TE-PGN-Ca-alginate beads into the cuvette containing reaction buffer and illuminating the stirred sample with a continuous wave NIR laser ($\lambda = 800 \pm 20$ nm, 15 W). Calcium-alginate beads (5) containing only nonconjugated *glk*^{AP}, reaction buffer, or pure Au nanorods were also analyzed as controls. The laser wavelength chosen for illumination was near the peak longitudinal plasmon resonance of the Au NR TE-PGN core (Figure 2D). An integrated water jacket of the cuvette, connected to a water bath/immersible pump, was used to maintain bulk reaction temperatures at standard conditions (*i.e.*, nonthermophilic, 35−50 °C). We chose working temperatures of 40−45 °C, since this range was just slightly cooler than the temperature range where Glk^{AP} displays a strong, exponentially temperature-dependent activity response (Figure 2C). Following laser irradiation, the samples were aliquoted and the reactions

quenched with EDTA and put on ice until they could be measured.

As seen in Figure 5A, laser-treated Ca-alginate beads encapsulating enzyme only (enzyme + alginate, left two bars) did not display any laser-dependent activity: the observed glucokinase activity matched the activity of bulk temperature controls. No activity was observed for NP-only and buffer-only Ca-alginate beads, as expected. In contrast, for the laser-irradiated TE-PGN Ca-alginate beads, the observed glucokinase activity substantially exceeded the analogous bulk temperature controls, showing a 60% increase (Figure 5A, Au NR + enzyme + alginate, right two bars). This laser-dependent increase in enzyme activity shows that Ca-alginate encapsulation of the complexes is critical to this response, most likely due to heat trapping by the alginate matrix, which assists in the formation of a temperature gradient around the illuminated NR−enzyme complexes.

To further investigate the role of the Ca-alginate matrix, catalytic amounts of unencapsulated enzyme or TE-PGNs (1/100 dilution, absorbance at 800 nm of 0.066) were tested under the same laser conditions
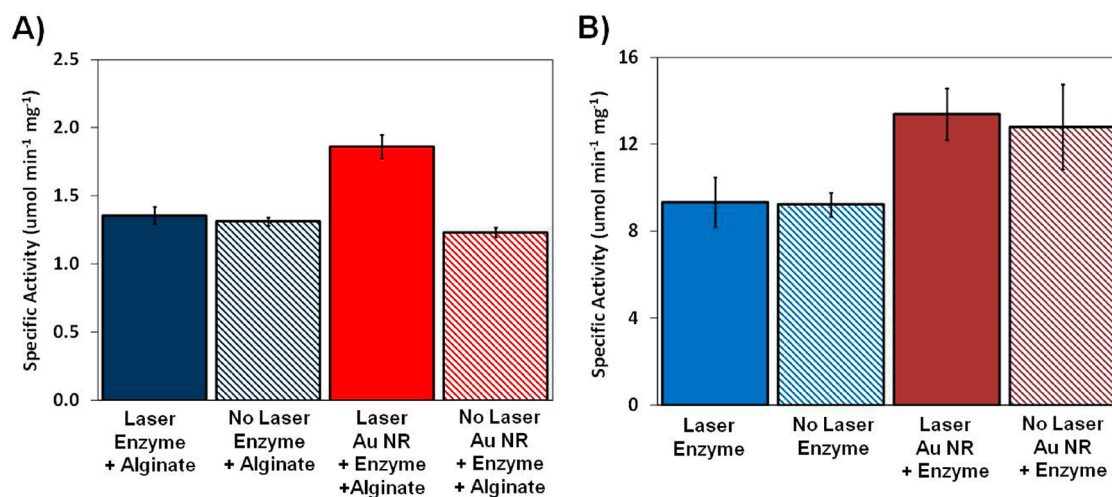
Figure 5. Laser response of the thermophilic enzyme—photothermal gold nanoparticles. (A) Specific activity of glucokinase Ca-alginate beads (enzyme + alginate) and the TE-PGN Ca-alginate beads (Au NR + enzyme + alginate) with laser irradiation *vs* no laser irradiation (respective bulk temperature controls). Five beads were used per reaction run. **(B)** Specific activity of unencapsulated glucokinase only (enzyme) and the TE-PGNs (Au NR + enzyme) with laser irradiation *vs* no laser irradiation (respective bulk temperature controls). For both panels, error bars denote the standard deviation from 3 replicates. Bulk temperatures were 42 °C for all enzyme experiments and 44 °C for all TE-PGN experiments. The laser power was 15 W for all laser irradiation experiments. Au NR-only and reaction buffer-only controls (with and without Ca-alginate) were also run, showing no laser-induced or bulk thermal activity (specific activities = 0).

as above. As seen in Figure 5B, no laser-dependent activation of the TE-PGNs was seen; both the laser-irradiated unbound enzyme (enzyme, left two bars) and TE-PGNs (Au NR + enzyme, right two bars) displayed the same specific activity as their respective bulk temperature controls. For the unencapsulated TE-PGNs, we suspect that a nanoscale temperature gradient was not being established (*i.e.*, the heat from the Au NR core surface is diffusing to the surrounding media such that Glk[AP] is not significantly activated[30]) (see Discussion).

DISCUSSION

In this study, we investigated the process of light-induced activation of a heat-responsive, thermophilic enzyme to remotely control a biochemical reaction while maintaining mesophilic bulk temperatures of ~20—50 °C. This is in contrast with some conventional photothermal applications where the photothermal response of Au nanoparticles is used for bulk heating.[1,7,16,31] To achieve our goal, we created thermophilic enzyme—photothermal gold nanoparticle complexes by conjugating a heat-responsive enzyme, *A. pernix* glucokinase, to plasmonic Au NRs, then encapsulating the TE-PGNs in a Ca-alginate matrix. Here the goal was to retain the photothermal heat generated from the Au NR cores such that the temperature around the NP surface is sufficient to activate the attached Glk[AP] peptides while bulk heating of the reactor volume was minimized. Ultimately, when the TE-PGN Ca-alginate beads were laser irradiated with a continuous wave laser, their glucokinase activity exceeded the analogous bulk temperature controls by 60%, showing validity of the light-activation concept.

Encapsulation of the TE-PGNs in Ca-alginate provided an initial means of validating our thermophilic enzyme—photothermal gold nanoparticles using a continuous wave laser amenable to industrial and practical applications. Two recent studies have successfully encapsulated unfunctionalized Au-NRs in Ca-alginate,[29,32] such that the desired properties of the Ca-alginate matrix and Au-NRs were retained. In one of these studies,[32] single Au NR Ca-alginate clusters were continuously irradiated and successfully heated from 25 °C to over 60 °C using a laser irradiation regime similar to that employed in this study. Importantly, the collective effect of heating nanoparticle clusters, similar to our conjugates encapsulated in calcium alginate, has been observed previously and provided local temperature increases of several tens of degrees over that of the bulk temperature.[33,34] For our observed 60% increase in glucokinase activity, it can be inferred from Figure 2C that, at a minimum, a ~20 °C temperature differential (*i.e.*, ~64 °C inside the beads) was achieved between the TE-PGN Ca-alginate bead and the bulk solution, approaching the 35 °C seen by Jo *et al.*[32] Our setup ensured that the encapsulated TE-PGNs remained submerged during the experiments, thus allowing uniform mass and heat transfer between the bead and the bulk water. The bulk temperature was observed to increase from 42 °C (water bath temperature) to 44 °C following laser irradiation of the encapsulated TE-PGNs.

We observed a 60% increase in glucokinase activation when the encapsulated TE-PGNs were laser irradiated, but the activation was below the maximum of ≥8-fold activation based on the activity *vs* temperature profiles (Figure 2C). The encapsulation does introduce

inherent complications that could limit enzyme activity, despite successful photothermal heating. For example, establishing a higher temperature gradient by sequestering the TE-PGNs together could have a negative impact on mass transfer of reactants and products. The separate ∼8-fold lower specific activity that the TE-PGN Ca-alginate beads display over the unencapsulated TE-PGNs in bulk thermal studies suggests this (see Figure 2A,C). However, these bulk thermal studies could also present heat transfer limitations, in that, here, the insulation effects of the Ca-alginate could work opposite the desired direction seen when photothermal heating occurs. However, we attempted to minimize this effect by allowing bulk thermal controls to equilibrate at the desired temperature. The lowered specific activity could also be compounded further during photothermal heating as the beads shrink somewhat due to an expulsion of air and water (which may also indicate inhibition of mass transfer of reactants to the enzymes). As stated earlier, the lower specific activity due to encapsulation would not be a significant drawback, since the Ca-alginate encapsulated beads are reusable multiple times.

The principal limitation of unencapsulated TE-PGNs in this application is the creation of a proper nanoscale temperature gradient originating from the gold surface, permitting enzyme activation. Theoretical and semiempirical modeling suggest that achieving a high temperature gradient (>10 °C) at the gold nanoparticle surface may require high optical densities, on the order of 10^4–10^5 W/cm^2.[7,31,35,36] Our experimental regime and use of a continuous wave laser at 15 W provides an optical density at least 1000-fold below this, which explains the lack of any observed laser-dependent activation without encapsulation. It should be noted that many conventional applications of Au nanoparticles (i.e., tumor treatment) are believed to exploit relatively small temperature gradients compared to the bulk temperature.[31,37] These sustained, albeit small, temperature gradients can rapidly produce high bulk temperatures if enough Au nanoparticles are irradiated. Since focusing the beam size down to micrometer levels is not desirable for a biochemical reactor application, the best approach for light-dependent activation of unencapsulated TE-PGNs may be to employ pulsed lasers sources.[36,38] However, use of such lasers provides unique challenges, as the pulse energy, duration, and frequency must be fine-tuned so that the gold−thiol bonds are not broken and the Au NR cores, as well as the attached proteins, are not fragmented.[38,39] Conversely, the pulses would have to be frequent enough to sustain a permanent temperature gradient, enabling the attached enzyme in the TE-PGNs to achieve and maintain an active conformation.

Encapsulation, which enables the use of a simple CW laser source, is appealing in its simplicity; however, our current fabrication method provides beads not amenable to in vivo use due to their size. Thus fabrication methods involving microfluidics, and/or other encapsulation materials, would be warranted to greatly reduce the current dimensions. Perhaps, more ideally, the encapsulation material could be eliminated and TE-PGN clusters could be possibly made through molecular−protein linkers to provide the needed heat generation using a CW laser with completely nanoscale materials. Future fine-tuning of all parameters including encapsulation materials/bead coating, heat generation/type of laser employed, transfer limitations, and mixing could significantly improve TE-PGN performance and eventually shrink our current system to the nanoscale for in vivo use.

CONCLUSION

Thermophilic enzyme−photothermal gold nanoparticle complexes have the potential to be used in a wide variety of ground-breaking applications. For example, TE-PGNs using a thermophilic polymerase (i.e., Taq polymerase) could further refine the concept of "laser-assisted" PCR.[40] Engineering TE-PGNs for the incorporation of thermophilic hydrogenases could take advantage of the thermodynamic benefits of elevated temperature (from the Gibbs equation $\Delta G = \Delta H - T\Delta S$) for the production of an important biofuel, H$_2$, under more standard nonthermophilic temperatures (≤50 °C).[41,42] Ultimately, remote light-driven control of an entire biological system could be achieved using TE-PGNs utilizing a global regulator after subsequent incorporation of TE-PGNs in vivo. With a plethora of thermophilic enzymes available and being discovered,[43] the applications are nearly limitless. Extension of this study to other thermophilic enzymes, materials, fabrication techniques, and/or lasers (such as pulsed) could result in the synthesis of additional TE-PGNs that would significantly change how biochemical pathways are studied and controlled in the future.

METHODS

Cloning of A. pernix Glk with N-Terminal Tags. Genomic DNA of A. pernix (NBRC 100138G) was obtained from NITE Biological Resource Center, Japan. PCR amplification of glk was performed with the primers 5-TACCATGGGTTGCGGTGGTCATCATCATCAT-CATCACGGTGGTGGTGTGGCGGAGGTTGTTGCT-3 and 5-GCAA-GCTTGCTGCTAGAAGATTGGGAGGT-3, in which the forward primer contained additional coding information for both a N-terminal cysteine (Cys) residue tag and a His$_6$ tag. After digestion of the ends with NcoI and HindIII (New England Biolabs; the PCR product was cloned into the pET28a expression vector (Novagen). After restriction and sequencing analysis, the resulting pET28a-cyshis$_6$glk^{AP} vector was transformed into the BL21(DE3) expression strain (Novagen). All techniques were performed according to the manufacturer or as previously described.[44,45]

Preparation of Cell Extracts and Purification of *A. pernix*-Tagged Glk. *E. coli* BL21(DE3) [pET28a-*cyshis_6glk*^{AP}] cells were aerobically grown in 75 mL of Luria−Bertani medium containing 40 μg/mL of kanamycin at 37 °C to an optical density at 600 nm of ∼0.8, at which expression of the *cyshis_6glk*^{AP} gene was initiated with the addition of 1 mM IPTG. After 3 h of further growth, the cells were pelleted (160 OD equivalents) by centrifugation at 4 °C and stored at −80 °C. Cell extracts were prepared from the pellets by cell disruption with a Disruptor Genie (Scientific Industries, Inc.) of cell suspensions in 4 mL of NPI-10 buffer (Qiagen) containing 5 mM β-mercaptoethanol (0.5 g glass beads + 1 mL cells in a 1.5 microcentrifuge tube, 4 total). After centrifugation (16000*g* for 10 min at 4 °C), the solution was heat precipitated at 85 °C for 25 min and centrifuged again at 4 °C. A near homogeneous Cys-His$_6$-Glk^{AP} enzyme preparation was achieved by use of affinity Ni-NTA resin spin columns at 15 °C according to the manufacturer's protocol for native conditions (Qiagen) with a final suspension volume of 400 μL in NPI-500. When necessary, dialysis against PBS buffer was performed once overnight at 4 °C to remove the imidazole using Slide-A-Lyzer dialysis cassettes (7000 MWCO, Thermo Scientific). If warranted, eluate was stored at 4 °C. Under these conditions, activity remained constant for several days. Protein concentration was determined by the use of the Lowry assay with BSA as the standard. Analysis of protein expression was performed *via* sodium dodecyl sulfate-polyacrylamide gel electrophoresis (SDS-PAGE) using NuPAGE Novex 12% Bis-Tris 10-well gels (Invitrogen), as described by the manufacturer. Once electrophoresis was completed, the gel was washed and stained with SimplyBlue SafeStain (Invitrogen), according to the manufacturer protocol.

Gold Nanorod Fabrication. *Materials Used for Au NR Synthesis.* Gold-(III) chloride trihydrate (HAuCl$_4$·3H$_2$O, 99%) and L-ascorbic acid (99+%) were purchased from Sigma-Aldrich. Cetyltrimethylammonium bromide (CTAB, ≥96%) was purchased from Fluka, and sodium borohydride (NaBH$_4$) was obtained from Acros. Silver nitrate (AgNO$_3$, ≥99%) was purchased from Strem Chemicals. Deionized water from a Barnstead NANOpure Diamond system (resistivity ≥ 18 MΩ/cm) was used for Au NR synthesis. All chemicals were used as-received unless otherwise noted.

Au NRs were synthesized using the method of Sau *et al.*[46] Briefly, a 127 mM HAuCl$_4$ stock solution was prepared by dissolving 5 g of HAuCl$_4$·3H$_2$O in 95 mL of water. A 0.01 M HAuCl$_4$ solution was prepared by diluting 0.79 mL of the HAuCl$_4$ stock solution with 9.21 mL of nanopure water. A stock 0.10 M CTAB solution was prepared by dissolving 2.19 g of CTAB with vigorous stirring and low heat in 60 mL of water. An ice-cold 0.01 M NaBH$_4$ solution was prepared by diluting an ice-cold 0.1 M NaBH$_4$ solution (0.038 g of NaBH$_4$ in 10 mL of ice-cold water). The Au seed sol was synthesized by adding 0.60 mL of ice-cold 0.01 M NaBH$_4$ to a vigorously stirred solution of 0.32 mM HAuCl$_4$ (0.25 mL of 0.01 M HAuCl$_4$ solution) and 96.8 mM CTAB (7.5 mL of 0.1 M CTAB). The seed sol was vigorously stirred for 2 min following addition of NaBH$_4$ and was stored in a 27 °C water bath for no more than 10 min. Au NR growth solution was prepared by first adding 0.30 mL of a 0.01 M AgNO$_3$ solution (0.017 g of AgNO$_3$ in 10 mL of water) to a gently stirred solution of 0.40 mM HAuCl$_4$ (2 mL of 0.01 M HAuCl$_4$ solution) and 96.0 mM CTAB (47.5 mL of 0.1 M CTAB). The resulting solution was vigorously stirred, and 0.32 mL of a 0.1 M ascorbic acid solution (0.18 g of ascorbic acid in 10 mL of water) was quickly added to make the final NR growth solution. The NR growth solution was equilibrated in a 27 °C water bath, and 0.38 mL of the Au seed sol was added. The resulting Au NR (Au NR) sol was gently stirred for ∼4 h at 27 °C. The final Au NR sol was washed twice by centrifuging at 12 000 rpm for 10 min. The cleaned sol was diluted such that the absorbance of the Au NR longitudinal surface plasmon (λ ∼770 nm) was 1.41.

Enzyme Functionalization of Au Nanorods. Conjugation of Cys-His$_6$-Glk^{AP} to the gold NRs was initiated immediately after Ni-NTA spin column elution (to prevent any disulfide bond formation). Briefly, 375 μL of extract was added to 1425 μL of NRs in a microcentrifuge tube, gently mixed, and placed in a rotisserie shaker overnight at room temperature. The next morning, the conjugates were pelleted at 13400*g* for 30 min, and the pellet was washed three times with 1 mL of PBS buffer

to remove all free, unbound enzyme. To resuspend the pellet, four brief sonication pulses were performed with a Branson Sonifier 250 at the lowest settings with a final suspension volume of between 50 and 200 μL. The resulting conjugates were kept at room temperature throughout the day with intermittent vortexing, where the activity remained constant.

Enzyme Entrapment in Calcium Alginate Beads. Cys-His$_6$-Glk^{AP} or the Cys-His$_6$-Glk^{AP}-functionalized Au NRs were entrapped in Ca-alginate beads by mixing equal volumes of the enzyme or conjugates with 1.5% w/v of medium-viscosity sodium alginate salt (MP Biomedicals, LLC). The mixture was vortexed, and 10 μL was pipetted and dropped into 15 mL of 0.5 M CaCl$_2$ solution at an appropriate height so that spherical Ca-alginate beads were formed. After a minimum of 10 min of hardening in the same solution, the CaCl$_2$ solution was removed and replaced with Tris buffer (pH 7.5). The beads were stable for at least several days.

Enzyme Assay for Glucokinase Activity and Laser Setup. The Cys-His$_6$-Glk^{AP} activity (glucose + ATP → G6P + ADP) was measured by coupling the ATP-dependent formation of glucose-6-phosphate (G6P) to the reduction of NADP$^+$ *via* G6P dehydrogenase (GPD) from yeast as previously reported.[20] Briefly, the initial assay mixture (500 μL) contained 100 mM Tris-HCl (pH 6.2, 90 °C), 5 mM glucose, 2 mM ATP, and 4 mM MgCl$_2$. After pre-incubation in a microcentrifuge tube, the reaction was started with the addition of the free enzyme, conjugates, or beads. This mixture was then incubated anywhere from 1 to 25 min at the temperature of interest or irradiated with the laser (see below), and the reaction was quenched by addition of EDTA to a final concentration of 10 mM and cooling in ice water for a minimum of 2 min. In the secondary reaction, the G6P concentration was quantified by addition of 0.6 mM NADP$^+$ and 0.5 units of GPD in 100 mM Tris (pH 7.5) to a final volume of 1 mL and incubation at 40 °C. The reduction of NADP$^+$ at 365 nm was determined 5 min later. This coupled assay was used as the basis for all activity work determined in this study.

For all laser studies and respective controls, a constant-temperature quartz cuvette (Starna Cells, Inc.) with a nominal volume of 825 μL (not including neck volume), a 13 mm sample chamber diameter, and a depth/path length of 10 mm, connected to a water bath/immersible pump when appropriate, was used. The laser utilized was an 800 ± 20 nm Diomed 15 Plus model. The end of the fiber was placed vertically above both focusing lenses and the cuvette (laid sideways, water surface tension in the neck prevented spillage) to provide a spot size the same as the cuvette window (power 15 W, spot size diameter = 13 mm, optical intensity = power/beam cross section = 11 W/cm^2). Temperatures were monitored by a thermocouple. Mixing was achieved with a 2 mm spherical stir bar placed in the cuvette spun with a magnetic stir plate at 1500 RPM (Sunset model, IKA Works). After laser treatment of 850−900 μL samples, a 500 μL aliquot was taken for each and processed as above for the thermal reactions. For a diagram of the laser setup see Figure 4.

Physical Characterization Methods. *Ultraviolet−Visible Spectroscopy.* The absorbance of cleaned Au NR sols and prepared Au NR−protein conjugates between wavelengths of 400 and 900 nm was measured on a Shimadzu UV-2401 PC spectrophotometer. Polystyrene cuvettes (Fischer Scientific) with a path length of 1 cm were used. Transmission Electron Microscopy: The length and width of Au NRs was determined using TEM images collected on a JEOL 2010 transmission electron microscope operating at 100 kV. The NR sol was deposited onto 200-mesh carbon/Formvar grids by evaporating a drop of sol at room temperature (23 °C). The number-average size distribution for each sample (width and length) was determined by measuring 400+ particles using ImageJ Software. Inductively Coupled Plasma Optical Emission Spectroscopy: ICP-OES (Perkin-Elmer Optima 4300 DV) of the AuNR−protein conjugates was used to determine the total Au concentration so that the AuNR:protein ratio of the conjugates could be calculated. AuNR−protein conjugates were dissolved in 2 mL of concentrated *aqua regia* for at least 1 h. The resulting solution was syringe-filtered (VWR 0.2 μm polypropylene) and diluted with water to a volume of 5 mL such that the total Au concentration was <20 ppm Au. Thermogravimetric Analysis (TGA): Thermogravimetric analysis of Au−protein conjugate calcium alginate

beads was done using a Q600 TA Instruments to verify water content in alginate beads. All TGA experiments were done using air (Matheson Trigas, flow rate = 40 mL/min) with a temperature ramp rate of 10 °C/min from ~30 to 700 °C. Scanning Electron Microscopy: The structure of TE-PGN Ca-alginate beads was analyzed using a JEOL 6500F scanning electron microscope with the electron gun operating at 15 kV. The beads were dried at 60 °C under vacuum, placed on an aluminum stub, and sputter-coated with 20 nm of Au prior to analysis.

Conflict of Interest: The authors declare no competing financial interest.

Supporting Information Available: Thermogravimetric analysis of alginate beads (Figure S1). Glucokinase specific activity values of Figure 5, shown in table format (Figure S2). This material is available free of charge via the Internet at http://pubs.acs.org.

REFERENCES AND NOTES

1. Huschka, R.; Zuloaga, J.; Knight, M. W.; Brown, L. V.; Nordlander, P.; Halas, N. J. Light-Induced Release of DNA from Gold Nanoparticles: Nanoshells and Nanorods. *J. Am. Chem. Soc.* **2011**, *133*, 12247–12255.
2. Bardhan, R.; Chen, W.; Bartels, M.; Perez-Torres, C.; Botero, M. F.; McAninch, R. W.; Contreras, A.; Schiff, R.; Pautler, R. G.; Halas, N. J.; *et al.* Tracking of Multimodal Therapeutic Nanocomplexes Targeting Breast Cancer In Vivo. *Nano Lett.* **2010**, *10*, 4920–4928.
3. Sharrna, P.; Brown, S.; Walter, G.; Santra, S.; Moudgil, B. Nanoparticles for Bioimaging. *Adv. Colloid Interface Sci.* **2006**, *123*, 471–485.
4. Huschka, R.; Neumann, O.; Barhoumi, A.; Halas, N. J. Visualizing Light-Triggered Release of Molecules inside Living Cells. *Nano Lett.* **2010**, *10*, 4117–4122.
5. Dreaden, E. C.; Alkilany, A. M.; Huang, X.; Murphy, C. J.; El-Sayed, M. A. The Golden Age: Gold Nanoparticles for Biomedicine. *Chem. Soc. Rev.* **2012**, *41*, 2740–2779.
6. Pallaoro, A.; Braun, G. B.; Moskovits, M. Quantitative Ratiometric Discrimination between Noncancerous and Cancerous Prostate Cells Based on Neuropilin-1 Overexpression. *Proc. Natl. Acad. Sci. U. S. A.* **2011**, *108*, 16559–16564.
7. Govorov, A. O.; Richardson, H. H. Generating Heat with Metal Nanoparticles. *Nano Today* **2007**, *2*, 30–38.
8. Alkilany, A. M.; Thompson, L. B.; Boulos, S. P.; Sisco, P. N.; Murphy, C. J. Gold Nanorods: Their Potential for Photothermal Therapeutics and Drug Delivery, Tempered by the Complexity of Their Biological Interactions. *Adv. Drug Delivery Rev.* **2012**, *64*, 190–199.
9. Guerrero-Martinez, A.; Grzelczak, M.; Liz-Marzan, L. M. Molecular Thinking for Nanoplasmonic Design. *ACS Nano* **2012**, *6*, 3655–3662.
10. Weissleder, R. A Clearer Vision for *In Vivo* Imaging. *Nat. Biotechnol.* **2001**, *19*, 316–317.
11. Turner, P.; Mamo, G.; Karlsson, E. N. Potential and Utilization of Thermophiles and Thermostable Enzymes in Biorefining. *Microb. Cell Fact.* **2007**, *6*, 9.
12. Sambrook, J.; Russell, D. W. Expression of Cloned Genes in *E. coli* Using IPTG-Inducible Promoters. *CSH Protocols.* **2006**, 1.
13. Stanley, S. A.; Gagner, J. E.; Damanpour, S.; Yoshida, M.; Dordick, J. S.; Friedman, J. M. Radio-Wave Heating of Iron Oxide Nanoparticles Can Regulate Plasma Glucose in Mice. *Science* **2012**, *336*, 604–608.
14. Schroeder, A.; Goldberg, M. S.; Kastrup, C.; Wang, Y.; Jiang, S.; Joseph, B. J.; Levins, C. G.; Kannan, S. T.; Langer, R.; Anderson, D. G. Remotely Activated Protein-Producing Nanoparticles. *Nano Lett.* **2012**, *12*, 2685–2689.
15. Lee, S. E.; Liu, G. L.; Kim, F.; Lee, L. P. Remote Optical Switch for Localized and Selective Control of Gene Interference. *Nano Lett.* **2009**, *9*, 562–570.
16. Miyako, E.; Nagata, H.; Hirano, K.; Hirotsu, T. Laser-Triggered Carbon Nanotube Microdevice for Remote Control of Biocatalytic Reactions. *Lab Chip* **2009**, *9*, 788–794.
17. Knecht, L. D.; Ali, N.; Wei, Y.; Hilt, J. Z.; Daunert, S. Nanoparticle-Mediated Remote Control of Enzymatic Activity. *ACS Nano* **2012**, *6*, 9079–9086.
18. Stehr, J.; Hrelescu, C.; Sperling, R. A.; Raschke, G.; Wunderlich, M.; Nichtl, A.; Heindl, D.; Kurzinger, K.; Parak, W. J.; Klar, T. A.; *et al.* Gold Nanostoves for Microsecond DNA Melting Analysis. *Nano Lett.* **2008**, *8*, 619–623.
19. Buchkremer, A.; Linn, M. J.; Reismann, M.; Eckert, T.; Witten, K. G.; Richtering, W.; von Plessen, G.; Simon, U. Stepwise Thermal and Photothermal Dissociation of a Hierarchical Superaggregate of DNA-Functionalized Gold Nanoparticles. *Small* **2011**, *7*, 1397–1402.
20. Hansen, T.; Reichstein, B.; Schmid, R.; Schonheit, P. The First Archaeal ATP-Dependent Glucokinase, from the Hyperthermophilic Crenarchaeon *Aeropyrum Pernix*, Represents a Monomeric, Extremely Thermophilic Rok Glucokinase with Broad Hexose Specificity. *J. Bacteriol.* **2002**, *184*, 5955–5965.
21. Nuzzo, R. G.; Zegarski, B. R.; Dubois, L. H. Fundamental-Studies of the Chemisorption of Organosulfur Compounds on Au(111). Implications for Molecular Self-Assembly on Gold Surfaces. *J. Am. Chem. Soc.* **1987**, *109*, 733–740.
22. Thierry, B. Drug Nanocarriers and Functional Nanoparticles: Applications in Cancer Therapy. *Curr. Drug Delivery* **2009**, *6*, 391–403.
23. Huang, H. C.; Koria, P.; Parker, S. M.; Selby, L.; Megeed, Z.; Rege, K. Optically Responsive Gold Nanorod-Polypeptide Assemblies. *Langmuir* **2008**, *24*, 14139–14144.
24. Solomon, K. V.; Moon, T. S.; Ma, B.; Sanders, T. M.; Prather, K. L. J. Tuning Primary Metabolism for Heterologous Pathway Productivity. *ACS Synth. Biol.* **2012**.
25. Harpaz, Y.; Gerstein, M.; Chothia, C. Volume Changes on Protein-Folding. *Structure* **1994**, *2*, 641–649.
26. Bhushan, I.; Parshad, R.; Qazi, G. N.; Gupta, V. K. Immobilization of Lipase by Entrapment in Ca-Alginate Beads. *J. Bioact. Compat. Polym.* **2008**, *23*, 552–562.
27. Gombotz, W. R.; Wee, S. F. Protein Release from Alginate Matrices. *Adv. Drug Delivery Rev.* **1998**, *31*, 267–285.
28. Fundueanu, G.; Nastruzzi, C.; Carpov, A.; Desbrieres, J.; Rinaudo, M. Physico-Chemical Characterization of Ca-Alginate Microparticles Produced with Different Methods. *Biomaterials* **1999**, *20*, 1427–1435.
29. Mitamura, K.; Imae, T.; Saito, N.; Takai, O. Fabrication and Structure of Alginate Gel Incorporating Gold Nanorods. *J. Phys. Chem. C* **2008**, *112*, 416–422.
30. Huehn, D.; Govorov, A.; Gil, P. R.; Parak, W. J. Photostimulated Au Nanoheaters in Polymer and Biological Media: Characterization of Mechanical Destruction and Boiling. *Adv. Funct. Mater.* **2012**, *22*, 294–303.
31. Richardson, H. H.; Carlson, M. T.; Tandler, P. J.; Hernandez, P.; Govorov, A. O. Experimental and Theoretical Studies of Light-to-Heat Conversion and Collective Heating Effects in Metal Nanoparticle Solutions. *Nano Lett.* **2009**, *9*, 1139–1146.
32. Jo, W.; Freedman, K.; Yi, D. K.; Bose, R. K.; Lau, K. K. S.; Solomon, S. D.; Kim, M. J. Photon to Thermal Response of a Single Patterned Gold Nanorod Cluster Under Near-Infrared Laser Irradiation. *Biofabrication* **2011**, 3.
33. Govorov, A. O.; Zhang, W.; Skeini, T.; Richardson, H.; Lee, J.; Kotov, N. A. Gold Nanoparticle Ensembles as Heaters and Actuators: Melting and Collective Plasmon Resonances. *Nanoscale Res. Lett.* **2006**, *1*, 84–90.

34. Hrelescu, C.; Stehr, J.; Ringler, M.; Sperling, R. A.; Parak, W. J.; Klar, T. A.; Feldmann, J. DNA Melting in Gold Nanostove Clusters. *J. Phys. Chem. C* **2010**, *114*, 7401–7411.

35. Baffou, G.; Quidant, R.; Javier Garcia de Abajo, F. Nanoscale Control of Optical Heating in Complex Plasmonic Systems. *ACS Nano* **2010**, *4*, 709–716.

36. Baffou, G.; Quidant, R.; Girard, C. Heat Generation in Plasmonic Nanostructures: Influence of Morphology. *Appl. Phys. Lett.* **2009**, 94.

37. Bardhan, R.; Lal, S.; Joshi, A.; Halas, N. J. Theranostic Nanoshells: From Probe Design to Imaging and Treatment of Cancer. *Acc. Chem. Res.* **2011**, *44*, 936–946.

38. Link, S.; Burda, C.; Nikoobakht, B.; El-Sayed, M. A. Laser-Induced Shape Changes of Colloidal Gold Nanorods Using Femtosecond and Nanosecond Laser Pulses. *J. Phys. Chem. B* **2000**, *104*, 6152–6163.

39. Braun, G. B.; Pallaoro, A.; Wu, G.; Missirlis, D.; Zasadzinski, J. A.; Tirrell, M.; Reich, N. O. Laser-Activated Gene Silencing *Via* Gold Nanoshell-Sirna Conjugates. *ACS Nano* **2009**, *3*, 2007–2015.

40. Kim, H.; Dixit, S.; Green, C. J.; Faris, G. W. Nanodroplet Real-Time PCR System with Laser Assisted Heating. *Opt. Express* **2009**, *17*, 218–227.

41. Baker, S. E.; Hopkins, R. C.; Blanchette, C. D.; Walsworth, V. L.; Sumbad, R.; Fischer, N. O.; Kuhn, E. A.; Coleman, M.; Chromy, B. A.; Letant, S. E.; *et al*. Hydrogen Production by a Hyperthermophilic Membrane-Bound Hydrogenase in Water-Soluble Nanolipoprotein Particles. *J. Am. Chem. Soc.* **2009**, *131*, 7508–7509.

42. Verhaart, M. R. A.; Bielen, A. A. M.; van der Oost, J.; Stams, A. J. M.; Kengen, S. W. M. Hydrogen Production by Hyperthermophilic and Extremely Thermophilic Bacteria and Archaea: Mechanisms for Reductant Disposal. *Environ. Technol.* **2010**, *31*, 993–1003.

43. Mehta, M. P.; Baross, J. A. Nitrogen Fixation at 92°C by a Hydrothermal Vent Archaeon. *Science* **2006**, *314*, 1783–1786.

44. Sambrook, J.; Russell, D. W., *Molecular Cloning: A Laboratory Manual*; Cold Spring Harbor Laboratory Press: New York, 2001.

45. Miller, J. H. *A Short Course in Bacterial Genetics: A Laboratory Manual and Handbook for Escherichia coli and Related Bacteria*; Cold Spring Harbor Laboratory Press: New York, 1992.

46. Sau, T. K.; Murphy, C. J. Seeded High Yield Synthesis of Short Au Nanorods in Aqueous Solution. *Langmuir* **2004**, *20*, 6414–6420.